Article

Trisaccharides of Phenolic Glycolipids Confer Advantages to Pathogenic Mycobacteria through Manipulation of Host-Cell Pattern-Recognition Receptors

Ainhoa Arbues, Wladimir Malaga, Patricia Constant, Christophe Guilhot, Jacques Prandi, and Catherine Astarie-Dequeker

ACS Chem. Biol., **Just Accepted Manuscript** • DOI: 10.1021/acschembio.6b00568 • Publication Date (Web): 22 Aug 2016

Trisaccharides of Phenolic Glycolipids Confer Advantages to Pathogenic Mycobacteria through Manipulation of Host-Cell Pattern-Recognition Receptors

Ainhoa Arbués [a,b], Wladimir Malaga [a,b], Patricia Constant [a,b], Christophe Guilhot [a,b], Jacques Prandi [a,b*] and Catherine Astarie-Dequeker [a,b*]

[a] CNRS, IPBS (Institut de Pharmacologie et de Biologie Structurale), BP 64182, 31077 Toulouse, France

[b] Université de Toulouse, UPS, 31077, Toulouse, France

supporting information

[*] *Corresponding authors*: C. Astarie-Dequeker, CNRS, IPBS (Institut de Pharmacologie et de Biologie Structurale), BP 64182, 205 route de Narbonne, F-31077 Toulouse Cedex 04, France. Phone : 33-561 17 54 55; Fax : 33-561 17 59 94; e-mail: Catherine.Astarie-Dequeker@ipbs.fr; J. Prandi , CNRS, IPBS, BP 64182, 205 route de Narbonne, F-31077 Toulouse Cedex 04, France. Phone: 33-561 17 54 85; Fax: 33-561 17 59 94; e-mail: Jacques.prandi@ipbs.fr.

Running title: Trisaccharides of PGLs: a weapon of pathogenic mycobacteria

Key words: Tuberculosis, leprosy, *Mycobacterium*, phenolic glycolipids, macrophages, immune responses, CR3, TLR2.

Abstract

Despite mycobacterial pathogens continue to be a threat for public health, the mechanisms that allow them to persist by modulating host immune response are poorly understood. Among the factors suspected to play a role are phenolic glycolipids (PGLs), produced notably by the major pathogenic species such as *Mycobacterium tuberculosis* and *Mycobacterium leprae*. Here, we reported an original strategy combining genetic reprogramming of the PGL pathway in *Mycobacterium bovis* BCG and chemical synthesis to examine whether sugar variations in the species-specific PGLs have an impact on pattern recognition receptors (PRRs) and the overall response of infected cells. We identified two distinct properties associated with the trisaccharide domains found in the PGLs from *M. leprae* and *M. tuberculosis*. First, the sugar moiety of PGL-1 from *M. leprae* is unique in its capacity to bind the lectin domain of complement receptor 3 (CR3) for efficient invasion of human macrophages. Second, the trisaccharide domain of the PGLs from *M. tuberculosis* and *M. leprae* share the capacity to inhibit Toll-like receptor 2 (TLR2)-triggered NF-κB activation, and thus the production of inflammatory cytokines. Consistently, PGL-1 was found to also bind isolated TLR2. By contrast, the simpler sugar domains of PGLs from *M. bovis* and *Mycobacterium ulcerans* did not exhibit such activities. In conclusion, the production of extended saccharide domains on PGLs dictates their recognition by host PRRs to enhance mycobacterial infectivity and subvert host immune response.

Pathogenic mycobacteria synthesize unique complex lipids that, being positioned at the outermost layer of their envelope, are able to interact with cells and serve as a tool to manipulate host immune response. Among the factors suspected to play a role are phenolic glycolipids (PGLs), which are produced by a limited number of mycobacterial species, notably the major human pathogens *Mycobacterium leprae*, *Mycobacterium tuberculosis* and *Mycobacterium ulcerans* –the aetiological agents of leprosy, tuberculosis and Buruli ulcer, respectively. In the case of *M. tuberculosis*, only a few strains synthetize PGL and this was shown to be associated with a hypervirulent phenotype in mice and rabbit (*1, 2*). Considering that very little is known about the interaction of these lipids with the host cell, a better understanding about their biological activity and molecular mechanism of action may contribute to novel therapeutic strategies against mycobacterial pathogens.

PGLs consist of a lipid core, a long-chain β-diol diesterified by polymethyl-branched fatty acids, which is well conserved with minor structural modifications (*3*). This core is ω-terminated by an aromatic nucleus that is glycosylated by a species-specific oligosaccharide (Figure 1). There is a large literature on the role of PGLs in the subversion of host immune response during mycobacterial infection (for review, see (*4*)). However, their molecular mechanisms of action are poorly known. Interestingly, their species-specific nature suggests that PGLs may be involved in functions unique to a given species. For instance, PGL-1 from *M. leprae* was reported to bind complement component C3 (*5*), with potential consequences on the capacity of *M. leprae* to invade host cells, and to subsequently affect bacterial resistance to intracellular killing by macrophages (*6-8*). PGL-1 was also proposed to modulate immune responses against *M. leprae* by suppressing the secretion of pro-inflammatory cytokines by monocytes/macrophages (*9, 10*) and the activation and proliferation of T lymphocytes (*11-13*). Yet, the latter effect is not restricted to PGL-1, since PGLs from several species inhibit non-specifically lymphoproliferative response to various stimuli (*12*). Moreover, PGLs from *M. marinum* (PGL-mar) and *M. tuberculosis* (PGL-tb) share the ability to abrogate the secretion of inflammatory cytokines (*1, 14, 15*), whereas PGL from *M. bovis* (PGL-bov) and phthiocerol dimycocerosates (DIM), the common lipid core, have no such effect (*1*). All together, these observations suggest that the biological activities of PGLs are primarily mediated by their species-specific saccharide domains. In line with this, Elsaidi and co-workers (*16-18*) have recently reported that subtle structural differences in the glycan portion of synthetic PGL analogues modulate the inhibition of the production of pro-inflammatory cytokines triggered by the pattern recognition receptor (PRR), Toll-like receptor 2 (TLR2). We speculate that PGLs act as pathogen-associated molecular patterns (PAMPs) and that sensing of their sugar moiety by PRRs on innate immune cells can trigger intracellular signalling cascades ultimately modulating the host microbicidal

response, as described for different types of glycosylated PAMPs such as β-glucan and lipopolysaccharides (*19*).

We previously reported that reprogramming of the PGL pathway in the vaccine strain *M. bovis* BCG to make it synthesize PGL-1 endows this bacterium with a better capacity to exploit complement receptor 3 (CR3) to invade human macrophages and subvert inflammatory responses (*10*). CR3, also named Mac-1, CD11b/CD18 or αMβ2 integrin, is a heterodimeric surface receptor expressed mainly on phagocytic cells that participates in cell invasion, activation, chemotaxis and cytotoxicity (*20*). Interestingly, CR3 was also found to function as a negative regulator of TLR-triggered inflammatory responses (*21, 22*). This receptor has the capacity to interact with a broad spectrum of ligands due to the presence of multiple binding sites in its α chain. Notably, a lectin-like domain that was characterized as a binding site for β-glucans, and thus representing a potential recognition site for the saccharide domain of PGLs (*23*).

The present study was designed to get new insights into the molecular mechanisms underlying PGL biological activities. To date, most studies addressing the role of PGLs employed either wild-type mycobacteria producing them or materials isolated from these organisms. We focused on their species-specific saccharide moieties using a cross-disciplinary approach, which combines their chemical synthesis and the genetic reprogramming of the model strain *M. bovis* BCG to make it synthesize PGLs produced by other mycobacterial pathogens in the context of a relevant mycobacterial envelope. We provide evidence now that trisaccharide moieties of the PGLs from *M. leprae* and *M. tuberculosis* act as PAMPs enabling these species to exploit host PRRs and consequently to enhance infectivity and to favour evasion of host immune responses.

RESULTS

Construction of recombinant BCG strains producing various species-specific PGLs

In previous work, we have extensively characterized the species-specific biosynthetic pathways of PGLs in mycobacteria (*10, 24*). This enabled us to pursue the genetic reprogramming of the PGL pathway in the model strain *M. bovis* BCG to make it synthesize the species-specific PGLs of other mycobacterial pathogens. BCG synthesizes a monosaccharide-containing PGL (PGL-bov) because of several genetic defects (*24*). Introduction of *M. tuberculosis* genes *Rv1511* (*gmdA*) and *Rv1512* (*epiA*), encoding proteins responsible for the transformation of the GDP-D-mannose in GDP-L-fucose, and a functional copy of *Rv2958c*, involved in the transfer of the second rhamnosyl residue, endows BCG with the capacity of synthesize the trisaccharide domain of PGL-tb (Figure 1 and 2A). Production of the PGLs from *M. ulcerans* (PGL-ulc) and PGL-1 requires first the disruption of

the *Rv2959c* ortholog, to avoid methylation of position 2 of the PGL-bov rhamnosyl residue. We previously showed that simultaneous introduction of *M. leprae* genes *ML0128* and *ML2348*, encoding for glycosyltransferases, together with the methyltransferase-encoding genes *ML012*6, *ML2346c* and *ML2347,* leads to the production of the trisaccharide residue characteristic of PGL-1 (*10*). Based on protein similarities, we identified *ML0126* as the gene encoding likely the methyltransferase catalysing methylation of the position 3 of the first rhamnosyl residue of PGL-1 (*10*). Therefore, to engineer BCG to make it synthesize PGL-ulc-like entities with a 3-*O*-methylrhamnose sugar residue, we transferred an integrative plasmid carrying the *ML0126* gene into *M. bovis* BCG *ΔRv2959c* (Figure 1 and 2B). The PGLs produced by the resulting recombinant strains were purified and the structure of their saccharide domains was characterized by NMR spectroscopy (Figure S1). The NMR analysis of PGL purified from rBCG ΔRv2959::ML0126 supported that the structure of the saccharide moiety corresponds to the expected 3-*O*-methyl-α-L-rhamnoside found in PGL-ulc and this was confirmed by comparison with its synthetic oligosaccharide (Figure S1). A replicative plasmid allowing the expression of *gfp* gene in mycobacteria was introduced in BCG and the various PGL-producing recombinant BCG (rBCG) strains in order to render them fluorescent. This transfer had no impact on the PGL production (Figure 2A).

Chemical synthesis of PGL oligosaccharide domains

We also aimed to investigate the activities of the saccharide domain of PGL devoid of the lipid core. For this purpose, we undertook to chemically synthesize these entities. The structures of the targeted oligosaccharide epitopes of the PGL (**OS-PGLs**) from *M. bovis*, *M. ulcerans*, *M. leprae* and *M. tuberculosis* are represented on Figure 1 (X = Me). All these epitopes share common α-linked L-rhamnopyranoside units which might be 2-*O*-methylated (PGL-bov and PGL-tb), 3-*O*-methylated (PGL-ulc and PGL-1) or 2,3-di-*O*-methylated (PGL-1). They can also be 2-*O*-glycosylated (PGL-1), 3-*O*-glycosylated (PGL-tb) or 4-*O*-glycosylated (PGL-1). Other species-specific features of the epitopes are the terminal 3,6-di-*O*-methyl-D-glucosyl residue of PGL-1 and the 2,3,4-tri-*O*-methyl-L-fucosyl residue found in PGL-tb.

Synthesis of the trisaccharidic epitope of PGL-1 have been described by Brennan (*25, 26*), Izumi (*27*) and more recently by the Lowary's group (*16*). The PGL-tb epitope was first prepared by Van Boom (*28*) and Fujiwara (*29*), and more recently by Scalan (*30*). The total synthesis of the whole PGL of *M. tuberculosis* has been achieved by Minnaard's group (*31*).

In our case, as all PGL epitopes were required, a convergent/divergent strategy was chosen with the different L-rhamnose units originating from a single advanced synthetic precursor**.** Compound **2**, the stannylene derivative of orthoester **1**, was found ideally suited for this purpose. After differential selective protections of the 3 and 4 positions of **2**, acidic opening of

the orthoester ring will introduce an acetate group on position 2 to secure the stereochemistry of all following glycosylations as α.

Preparation of the building blocks (Figure 3)

Differentiation of the 3 and 4 positions of **2** was obtained by selective methylation (or benzylation) of the position 3 of stannylene **2** and later introduction on position 4 of a protecting group, benzyl or silyl, orthogonal to the one previously put on position 3. This strategy was straightforward and gave access to all needed rhamnosyl donors **3**-**6** in three to five steps from orthoester **1**. Finally, the last glycosyl units needed for the elaboration of all OS-PGLs, 2,3,4-tri-*O*-methyl-L-fucosyl thioglycoside **7** and 3,6-di-*O*-methyl-D-glucosyl imidate **8** were prepared by slight modifications of reported procedures (*32, 33*).

Stannylene **2** was prepared from diol **1** and one equivalent of dibutyltinoxide in refluxing toluene with elimination of water. Selective 3-*O*-benzylation of **2** was carried out under standard conditions with benzyl bromide and tetrabutylammonium bromide in dimethylformamide (DMF) at 40°C (*34*). After workup, the crude product was silylated with tert-butyldimethylsilyl chloride (TBDMSCl) in pyridine to give orthoester **9** in 58% isolated yield for the two steps. Introduction of the anomeric trichloroacetimidate was done in two steps, acidic hydrolysis of the orthoester was followed by treatment of the hemiacetal with trichloroacetonitrile and 1,8-diazabicyclo[5.4.0]undec-7-ene (DBU) in dichloromethane (DCM). Compound **5** was isolated in 90% yield after these two steps. The very same strategy was used for preparation of donors **3** and **4**. Stannylene **2** was first selectively methylated on the 3 position using methyl iodide and tetrabutylammonium bromide in DMF at 40°C. However, the intermediate 3-*O*-methyl orthoester **10** was found to be highly volatile, excluding its isolation, even in a crude form. The reaction mixture was thus filtered on silica (THF elution) and THF was evaporated in the cold. The resulting solution of **10** in DMF was directly used for benzylation (excess NaH, BnBr, 0°C) to give known orthoester **11** in a 72% yield for the two steps (*35*). In a similar manner, treatment of the DMF solution of crude **10** with an excess of TBDMSCl in presence of imidazole gave the 4-*O*-silyl orthoester **12** in 64% yield from **2**. The two orthoesters **11** and **12** were then transformed to the corresponding trichloroacetimidates according to the sequence use above for **5**, known imidates **3** (*36*) and **4** (*37*) were efficiently obtained in respective yields of 77% and 68%.

The last rhamnosyl donor **6** was obtained in three steps from orthoester **1**. Benzylation of the 3 and 4 positions of **1** afforded dibenzyl orthoester **13** in 90% isolated yield (*38*). Introduction of the activable anomeric imidate was done as above and donor **6** was obtained in 77% from **13** (*39*).

Elaboration of the epitopes of PGLs (Figure 4)

OS-PGL-bov. The synthesis of this epitope started from imidate **6**. Glycosylation of a slight excess of *p*-cresol with **6** (cat. TMSOTf, DCM, –20°C) gave α-glycoside **14** in 73% yield. The

acetate group of **14** was removed under basic methanolic conditions, and alcohol **15** was then methylated with sodium hydride and methyl iodide in THF to give **16**. Overall yield for these two steps was 65%. Deprotection of **16** by hydrogenolysis (H_2, $Pd(OH)_2/C$) gave **OS-PGL-bov** in 95% yield.

OS-PGL-ulc and **OS-PGL-1.** The synthesis of **OS-PGL-ulc** and **OS-PGL-1** shares the same two first steps**.** Glycosylation (cat. TMSOTf, DCM, –20°C) of *p*-cresol with rhamnosyl donor **3** gave α-rhamnoside **17** in 72% yield and removal of the acetate group of **17** gave alcohol **18** in 90%. From **18**, **OS-PGL-ulc** was obtained in quantitative yield after hydrogenolysis (H_2, $Pd(OH)_2/C$) of the benzyl protecting groups.

For the elaboration of **OS-PGL-1, 18** was glycosylated with **4** and gave α-dirhamnoside **19** in 75% yield. Introduction of the 2'-*O*-methyl group on **19** was done in two steps as described above for the preparation of **OS-PGL-bov** and **21** was obtained in 78% yield from **19.** Deprotection of the 4'-*O*-silyl group of **21** was done with tetrabutylammonium fluoride (NBu_4F) in THF and alcohol **22** was isolated in 85% yield. Final glycosylation of **22** with glucosyl donor **8** gave trisaccharide **23** in 91% yield as a single β-anomer on the new anomeric center. Deprotection of **23** to **OS-PGL-1** was done in two steps (MeONa, MeOH, then H_2, $Pd(OH)_2/C$, AcOEt/MeOH) and **OS-PGL-1** was isolated in 65%.

OS-PGL-tb. As the two L-rhamnopyranoside units of the PGL-tb are glycosylated on position 3, only one rhamnose building block **5** was needed for the synthesis of this epitope. Glycosylation of *p*-cresol with **5** gave pure α-L-rhamnopyranoside **24** in 68% yield. Introduction of the 2-*O*-methyl group on **24** was done in two steps as described above for **OS-PGL-bov** and **26** was obtained in 78% yield. Selective unmasking of the 3 position of **26** was carried out by hydrogenolysis and gave alcohol **27** in 93% yield. Glycosylation of **27** with imidate **5** gave α-dirhamnoside **28** in 89% yield and the 3'-*O*-benzyl protecting group of the non-reducing rhamnose unit was removed by catalytic hydrogenation to give alcohol **29** in 95% yield. Glycosylation of this disaccharide with thiofucoside **7** (N-iodosuccinimide, cat. TMSOTf, CH_2Cl_2, –20 °C to room temperature) gave trisaccharide **30** in good yield (70%). Final deprotection was carried out by treatment of **30** with sodium methanolate in methanol followed by reaction with NBu_4F in THF. The requested epitope **OS-PGL-tb** was isolated in 67% yield. All physico-chemical data for new compounds are described in the Supporting Information.

PGL-1 from *M. leprae* is unique to confer BCG with increased capacity to exploit CR3 lectin domain

Once the microbiological and molecular tools were generated, we undertook the comparison of the biological activities of the various PGLs. We have previously demonstrated that PGL-1

production endows rBCG with increased capacity to infect human macrophages (hMDM) (*10*). Therefore, we examined the role of other species-specific PGLs in this phenotype. After 2h of contact under non-opsonic conditions, all the strains were found to be efficiently phagocytosed (Figure 5A). Comparative analysis showed that rBCG expressing PGL-tb and PGL-ulc infected cells to the same extent as BCG, but we observed a marked increase in the percentage of hMDM infected by rBCG-PGL-1 (Figure 5A). These data confirm that expression of PGL-1 specifically enhances invasivity of rBCG and argue in favour of a critical role of the unique trisaccharide residue of PGL-1 in this phagocytosis process.

Next, we assessed whether the lectin domain of CR3 was involved in the PGL-1-mediated phagocytosis. hMDM were pre-treated with blocking antibodies (Ab) raised against either an undetermined extracellular region (2LPM19c) or the lectin domain (VIM12) of human CR3, and their impact on the differential uptake of BCG and rBCG-PGL-1 was subsequently evaluated (Figure 5B). In agreement with our previous results, none of the two Ab was able to affect the phagocytosis of BCG (*10*). By contrast, both of them significantly decreased the uptake of rBCG-PGL-1 in a specific manner, since no effect was observed with the isotype control. Interestingly, blockade of CR3 lectin domain restored phagocytosis of rBCG-PGL-1 at a level comparable to that observed with BCG (Figure 5B). Taken together, these results strongly support that PGL-1, through its species-specific sugar moiety, confers to BCG the capacity to exploit the lectin site of CR3 for a more efficient invasion of macrophages. Remarkably, this capacity was not shared by the other species-specific PGLs.

Lyn is critical in PGL-1-mediated increase of phagocytosis by hMDM

To our knowledge, the signalling process of the lectin domain of CR3 is poorly known but it is well known that the tyrosine kinases of the Src and Syk families contribute to initiate the integrin signalling pathway (for review, see (*40*)). In addition, Syk and the Src kinase Lyn have been shown to be required for the complement-mediated phagocytosis of pathogens (*22, 41*). To test whether these kinases are involved in the differential uptake of BCG and rBCG-PGL-1, we selectively knocked them down by siRNA-mediated gene silencing (*42*) (Figure 6A). When compared to siRNA control, Lyn and Syk knockdown did not impair the uptake of BCG by hMDMs (Figure 6B). By contrast, Lyn, but not Syk, inactivation greatly altered rBCG-PGL-1 uptake, providing evidence that only Lyn is required for the increase of CR3-mediated phagocytosis induced by PGL-1.

The unique sugar moiety in PGL-1 confers its capacity to specifically bind CR3

Our results of the phagocytosis experiments support the recognition of PGL-1 through the lectin domain of CR3. However, evidence demonstrating the direct binding were still missing. We developed a solid phase assay in which increasing concentrations (0.5–25 μM) of

isolated PGL-1 were incubated with immobilized human CR3. Bound PGL-1 was detected using an Ab specific for PGL-1 saccharide domain. Using this assay, we showed that native PGL-1, purified from *M. leprae*-infected armadillos, specifically binds human CR3 in a dose-dependent manner (Figure 7A). By contrast, no binding was detected when a non-relevant protein was coated into the plate wells (No CR3). Next, we wondered if PGL-1 sugar moiety was sufficient for CR3 recognition. Immobilized CR3 was incubated with either 5 μM purified PGL-1 or 50 μM OS-PGL-1. Detection using anti-PGL-1 Ab showed that both molecules were able to bind CR3 (Figure 7B). However, the binding observed for OS-PGL-1 was lower than for native PGL-1, even when used at a ten-fold higher concentration, suggesting that the lipid core enhances the affinity of CR3 for the PGL-1 saccharide epitope.

Since PGL-1 was the only PGL inducing an increase in the CR3-dependent uptake of rBCG by hMDM, we asked whether the direct binding to CR3 was also specific of PGL-1 sugar moiety. CR3 is a remarkably versatile receptor recognizing both endogenous ligands as well as microbial molecules due to the presence of two binding domains (*20*). The binding of non-protein ligands to CR3 is thought to be mediated by its lectin domain, which recognizes several sugars including yeast β(1→3)-glucans at highest affinity (*23*). Of note, the specific terminal disaccharide of PGL-1 contains a β(1→3)-linked glucose that may be crucial for the interaction with CR3 lectin domain. Since specific Abs for each PGL were not available, we developed a competition assay to address this question. CR3 was pre-incubated with the various synthetic OS-PGLs (50 μM) before being added to wells coated with purified PGL-1. Bound CR3 was subsequently detected using an Ab raised against CD11b. As predicted, the binding of CR3 to coated PGL-1 was dramatically reduced only in the presence of the synthetic PGL-1 saccharide moiety (Figure 7C). Taken together, these results clearly established that the specific interaction with CR3 is mediated by direct binding of the trisaccharide domain to this receptor.

Synthetic epitopes of PGL-1 and PGL-tb inhibit TLR2-dependent NF-κB activation

Next, we investigated the molecular mechanisms involved in the immunomodulatory properties of some of the PGLs produced by mycobacterial pathogens. We previously reported that PGL-1 production endows rBCG with a higher capacity to dampen inflammatory responses in infected macrophages (*10*). This prompted us to examine the role of other species-specific PGLs. First, we used a NF-κB-reporter THP-1 cell line designed to monitor activation of the nuclear factor Kappa B (NF-κB), a transcription factor controlling the expression of multiple inflammatory genes. After 16h of infection, BCG induced a strong increase of the mean Abs_{630nm} value indicative of expression of the reporter gene. In comparison with BCG, while infection with rBCG-PGL-ulc induced a similar response, the

response induced by rBCG-PGL-tb or rBCG-PGL-1 tended to be lower or significantly diminished (Figure 8A). We further monitored the level of the pro-inflammatory cytokine TNF-α in the supernatant of hMDM infected with BCG compared to that of rBCG expressing PGL-1 or PGL-tb. After 2h of infection, we confirmed that rBCG-PGL-1 induced less secretion of TNF-α than BCG (Figure 8B), despite the fact that it is more efficiently internalized (Figure 5A) (*10*). Similarly, infection with rBCG-PGL-tb led to relatively lower TNF-α secretion when compared to BCG (Figure 8B). These results indicate that PGL-1 and, to a lesser extent, PGL-tb share the capacity to dampen the secretion of TNF-α, in agreement with previous studies (*1, 10*), and strongly support the hypothesis that the immunosuppressive effects of PGLs require trisaccharide moieties (*18*).

To further explore this hypothesis, we tested the effect of purified PGLs and synthetic PGL epitopes in NF-kB activation. None of the tested compounds have an effect by themselves (data not shown). Recently, Elsaidi and co-workers established that truncated analogues of the PGLs produced by *M. leprae* and *M. tuberculosis*, but not *M. bovis*, inhibit the release of cytokines induced by TLR2 (*16, 17*), a PRR that promotes the synthesis of pro-inflammatory cytokines through the activation of NF-κB. This prompted us to evaluate the impact of isolated compounds on cells simultaneously treated with a TLR2 agonist, Pam3CSK4. As expected, this positive control induced a marked activation of NF-κB (Figure 8C). Addition of 5 μM purified PGL-1 dramatically decreased Pam3CSK4-induced activation of NF-κB, whereas 10 μM DIM, the common lipid core, had no such effect (Figure 8C). When 50 μM synthetic OS-PGLs were tested in the same system, we found that only the trisaccharide moieties of PGL-tb and PGL-1 were able to inhibit TLR2-dependent NF-κB activation (Figure 8C), and thus supporting the results published by Elsaidi and co-workers (*16-18*). However, since hMDM and THP-1 cells express a large repertoire of receptors, we cannot distinguish if trisaccharide-containing PGLs exert their inhibitory effect *via* a direct recognition by TLR2, or through potential crosstalk with another receptor recognizing the PGLs. Thus, we decided to switch to a HEK reporter cell line expressing only human TLR2. Cells were treated for 16h with 10 mg ml^{-1} Pam3CSK4 in addition to purified DIM (10 μM), purified PGL-1 (5 μM), or the synthetic OS-PGLs (50 μM). Similar to the results obtained in THP-1 cells, native PGL-1 and saccharide epitopes of PGL-tb and PGL-1 were found to inhibit NF-κB activation triggered by Pam3CSK4 (Figure 8D). This observation led us to propose that recognition by TLR2 mediates, at least partially, the inhibition of NF-κB activation induced by trisaccharide-containing PGLs. In line with this, purified PGL-1 was found to also bind immobilized human TLR2 in a solid phase assay (Figure 8E). Collectively, these results evidence that PGLs from *M. leprae* and *M. tuberculosis* can act as ligands of TLR2 to antagonize the signalling pathway downstream this receptor, and thus to dampen TNF-α secretion. Furthermore, we

showed that the down-regulation of TNF-α secretion is mediated in part by the trisaccharide, but not the monosaccharide epitopes of PGLs, through an inhibition of TLR2-dependent NF-κB activation. This is consistent with the capacity of both PGL-tb and PGL-1 to inhibit the secretion of monocyte chemoattractant protein-1 (MCP-1/CCL2) by macrophages (*1, 16*), unlike the effect induced by the PGL-mar, a PGL-ulc-like, in the zebrafish model that is TLR-independent (*43*). Despite the fact that DIM alone showed no activity, native PGL-1 was a ten-times more potent inhibitor than its corresponding saccharide epitope. These results suggest that the sugar domain is responsible for the specificity of TLR2 for some of the PGLs, which is determined by the length of the oligosaccharide; whereas the common lipid core would rather enhance the affinity of the receptor for the trisaccharide epitope, for example, by improving its presentation. This could be explained by the presence of several binding sites in TLR2 involved in the recognition of PGL; for instance, one sensitive to the length of the saccharide domain and that confers the species-specificity, and another one with a hydrophobic pocket to accommodate the lipid chains present in both whole PGL and lipopeptides–TLR2 favourite ligands.

We previously described a critical role of CR3 in the down modulation of TNF-α secretion induced by rBCG-PGL-1 when compared to BCG (*10*). While little is known about how the engagement of CR3 by a pathogen can mediate regulation of TLR-dependent signaling pathways, a recent study shows that TLR2-dependent pro-inflammatory responses can be down modulated by a negative feedback, which engages CR3 and a downstream signaling pathway including Lyn kinase (*22, 41*). To assess the role of Lyn in mediating immune suppression pathway(s) during the phagocytosis of rBCG-PGL-1, we selectively inactivated it by siRNA-mediated gene silencing and quantified TNF-α secretion. Lyn knockdown decreased TNF-α secretion by both BCG and rBCG-PGL-1-infected cells (Figure 8F). Nevertheless, this had no impact on the capacity of rBCG-PGL-1 to dampen TNF-α production in comparison with BCG (Figure 8F). Thus, under these conditions, engagement of Lyn in the phagocytic process did not contribute to CR3-mediated immune suppression and crosstalk with the TLR2 signaling pathway (*22*). Whether PGL-1 expression engages a crosstalk between CR3 and TLR2 for the modulation of pro-inflammatory cytokines remains an open question, but we clearly demonstrated that PGL-1 dampens TLR2 signalling independently of its capacity to engage CR3 in bacterial uptake.

This study demonstrates that trisaccharide moieties of PGL from *M. leprae* and *M. tuberculosis* act as PAMPs to enable bacteria to exploit host PRRs and subsequently modulate the host immune response. Their surface expression enhances pathogen infectivity through recognition of the lectin site of CR3 and also inhibits TLR2-dependent signaling cascades, by directly binding TLR2, that ultimately favors the resilience of *M. tuberculosis*

and *M. leprae* to subvert the hostile environment pose by the host cell. This report adds to the growing body of data indicating that *M. tuberculosis* is equipped with surface molecules aimed to inhibit TLR-orchestrating innate defences.

METHODS

An extended methods section describing assays for lipids purification, synthesis of PGL epitope, microbiology (bacterial growth conditions, biochemical analysis) and cell biology (culture conditions, reagents, siRNA transfection, quantification of NF-κB activity and TNF-α secretion and Western blot studies) can be found in the Methods section of the Supporting Information.

ACKNOWLEDGEMENTS

We are grateful to L. Blanc, C. Robert and J. Nigou (IPBS, Toulouse, France) for HEK and THP-1 experiments, to A. Benard (IPBS, Toulouse, France) for his help with ELISA, and G. Lugo-Villarino (IPBS, Toulouse, France) for his contribution to siRNA-mediated gene silencing and proof-reading of this manuscript. PGL-1 purified from *M. leprae* as well as antibodies against PGL-1 were provided by BEI resources. We thank the Genotoul plateforms TRI (IPBS, Toulouse, France) for the use of epifluorescence microscope. We thank A. Lemassu and M. Daffé (IPBS, Toulouse, France) for access to the various apparatus and the help with the structural characterization of glycolipids. AA is recipient of a fellowship from a European Research Grant of Marie Skłodowska-Curie actions (PIEF-GA-2012-329818). This work was supported by the Centre National de la Recherche Scientifique (CNRS), the National Research Agency (ANR-11-BSV3-001)) and by European Regional Development Funds.

CONFLICT OF INTEREST

The authors declare no conflict of interest.

AUTHORS CONTRIBUTION

Author contributions: AA designed and conducted *in vitro* and *ex-vivo* experiments and analyzed the results. WM carried out constructions of plasmid and recombinant strains. JP designed experiments and performed chemical synthesis. PC performed structural biochemistry experiments. CAD designed experiments and performed some ex-vivo experiments and analyzed data. CG and CAD conceived the project and obtained financial

support from ANR. AA, JP, CG and CAD wrote the paper. All authors reviewed the results and approved the final version of the manuscript.

REFERENCES

1. Reed, M. B., Domenech, P., Manca, C., Su, H., Barczak, A. K., Kreiswirth, B. N., Kaplan, G., and Barry, C. E., 3rd. (2004) A glycolipid of hypervirulent tuberculosis strains that inhibits the innate immune response, *Nature 431*, 84-87.
2. Tsenova, L., Ellison, E., Harbacheuski, R., Moreira, A. L., Kurepina, N., Reed, M. B., Mathema, B., Barry, C. E., 3rd, and Kaplan, G. (2005) Virulence of selected Mycobacterium tuberculosis clinical isolates in the rabbit model of meningitis is dependent on phenolic glycolipid produced by the bacilli, *J Infect Dis 192*, 98-106.
3. Daffe, M., and Laneelle, M. A. (1988) Distribution of phthiocerol diester, phenolic mycosides and related compounds in mycobacteria, *J Gen Microbiol 134*, 2049-2055.
4. Neyrolles, O., and Guilhot, C. (2011) Recent advances in deciphering the contribution of Mycobacterium tuberculosis lipids to pathogenesis, *Tuberculosis (Edinb) 91*, 187-195.
5. Schlesinger, L. S., and Horwitz, M. A. (1991) Phenolic glycolipid-1 of Mycobacterium leprae binds complement component C3 in serum and mediates phagocytosis by human monocytes, *J Exp Med 174*, 1031-1038.
6. Neill, M. A., and Klebanoff, S. J. (1988) The effect of phenolic glycolipid-1 from Mycobacterium leprae on the antimicrobial activity of human macrophages, *J Exp Med 167*, 30-42.
7. Chan, J., Fujiwara, T., Brennan, P., McNeil, M., Turco, S. J., Sibille, J. C., Snapper, M., Aisen, P., and Bloom, B. R. (1989) Microbial glycolipids: possible virulence factors that scavenge oxygen radicals, *Proc Natl Acad Sci U S A 86*, 2453-2457.
8. Launois, P., Blum, L., Dieye, A., Millan, J., Sarthou, J. L., and Bach, M. A. (1989) Phenolic glycolipid-1 from M. leprae inhibits oxygen free radical production by human mononuclear cells, *Res Immunol 140*, 847-855.
9. Silva, C. L., Faccioli, L. H., and Foss, N. T. (1993) Suppression of human monocyte cytokine release by phenolic glycolipid-I of Mycobacterium leprae, *Int J Lep Other Mycobact Dis 61*, 107-108.
10. Tabouret, G., Astarie-Dequeker, C., Demangel, C., Malaga, W., Constant, P., Ray, A., Honore, N., Bello, N. F., Perez, E., Daffe, M., and Guilhot, C. (2010) Mycobacterium leprae phenolglycolipid-1 expressed by engineered M. bovis BCG modulates early interaction with human phagocytes, *PLoS Pathog 6*, e1001159.
11. Mehra, V., Brennan, P. J., Rada, E., Convit, J., and Bloom, B. R. (1984) Lymphocyte suppression in leprosy induced by unique M. leprae glycolipid, *Nature 308*, 194-196.

12. Fournie, J. J., Adams, E., Mullins, R. J., and Basten, A. (1989) Inhibition of human lymphoproliferative responses by mycobacterial phenolic glycolipids, *Infect Immun 57*, 3653-3659.

13. Dagur, P. K., Sharma, B., Upadhyay, R., Dua, B., Rizvi, A., Khan, N. A., Katoch, V. M., Sengupta, U., and Joshi, B. (2012) Phenolic-glycolipid-1 and lipoarabinomannan preferentially modulate TCR- and CD28-triggered proximal biochemical events, leading to T-cell unresponsiveness in mycobacterial diseases, *Lipids Health Dis 11*, 119.

14. Sinsimer, D., Huet, G., Manca, C., Tsenova, L., Koo, M. S., Kurepina, N., Kana, B., Mathema, B., Marras, S. A., Kreiswirth, B. N., Guilhot, C., and Kaplan, G. (2008) The phenolic glycolipid of Mycobacterium tuberculosis differentially modulates the early host cytokine response but does not in itself confer hypervirulence, *Infect Immun 76*, 3027-3036.

15. Robinson, N., Kolter, T., Wolke, M., Rybniker, J., Hartmann, P., and Plum, G. (2008) Mycobacterial phenolic glycolipid inhibits phagosome maturation and subverts the pro-inflammatory cytokine response, *Traffic 9*, 1936-1947.

16. Elsaidi, H. R., Barreda, D. R., Cairo, C. W., and Lowary, T. L. (2013) Mycobacterial phenolic glycolipids with a simplified lipid aglycone modulate cytokine levels through Toll-like receptor 2, *Chembiochem 14*, 2153-2159.

17. Elsaidi, H. R., and Lowary, T. L. (2014) Inhibition of cytokine release by mycobacterium tuberculosis phenolic glycolipid analogues, *Chembiochem 15*, 1176-1182.

18. Elsaidi, H. R., and Lowary, T. L. (2015) Effect of phenolic glycolipids from *Mycobacterium kansasii* on proinflammatory cytokine release. A structure-activity relationship study, *Chem Sci 6*, 3161-3172.

19. Mahla, R. S., Reddy, M. C., Prasad, D. V., and Kumar, H. (2013) Sweeten PAMPs: Role of Sugar Complexed PAMPs in Innate Immunity and Vaccine Biology, *Front Immunol 4*, 248.

20. Ehlers, M. R. (2000) CR3: a general purpose adhesion-recognition receptor essential for innate immunity, *Microbes Infect 2*, 289-294.

21. Han, C., Jin, J., Xu, S., Liu, H., Li, N., and Cao, X. (2010) Integrin CD11b negatively regulates TLR-triggered inflammatory responses by activating Syk and promoting degradation of MyD88 and TRIF via Cbl-b, *Nature Immunol 11*, 734-742.

22. Dai, S., Rajaram, M. V., Curry, H. M., Leander, R., and Schlesinger, L. S. (2013) Fine tuning inflammation at the front door: macrophage complement receptor 3-mediates phagocytosis and immune suppression for Francisella tularensis, *PLoS Pathog 9*, e1003114.

23. Thornton, B. P., Vetvicka, V., Pitman, M., Goldman, R. C., and Ross, G. D. (1996) Analysis of the sugar specificity and molecular location of the beta-glucan-binding lectin site of complement receptor type 3 (CD11b/CD18), *J Immunol 156*, 1235-1246.

24. Malaga, W., Constant, P., Euphrasie, D., Cataldi, A., Daffe, M., Reyrat, J. M., and Guilhot, C. (2008) Deciphering the genetic bases of the structural diversity of phenolic glycolipids in strains of the Mycobacterium tuberculosis complex, *J Biol Chem 283*, 15177-15184.

25. Fujiwara, T., Hunter, S. W., Cho, S. N., Aspinall, G. O., and Brennan, P. J. (1984) Chemical synthesis and serology of disaccharides and trisaccharides of phenolic glycolipid antigens from the leprosy bacillus and preparation of a disaccharide protein conjugate for serodiagnosis of leprosy, *Infect Immun 43*, 245-252.

26. Chatterjee, D., Cho, S. N., Stewart, C., Douglas, J. T., Fujiwara, T., and Brennan, P. J. (1988) Synthesis and immunoreactivity of neoglycoproteins containing the trisaccharide unit of phenolic glycolipid I of Mycobacterium leprae, *Carbohydr Res 183*, 241-260.

27. Fujiwara, T., and Izumi, S. (1987) Synthesis of the neoglycoconjugates of the phenolic glycolipid-related trisaccharides for the serodiagnosis of leprosy, *Agric Biol Chem 51*, 2539-2547.

28. Veeneman, G. H., Van Leeuwen, S. H., Zuurmond, H., and Van Boom, J. H. (1990) Synthesis of carbohydrate-antigenic structures of Mycobacterium tuberculosis using an iodonium ion promoted glycosidaton approach, *J Carbohydr Chem 9*, 783-796.

29. Fujiwara, T. (1991) Synthesis of the trisaccharide-protein conjugate of the phenolic glycolipid of Mycobacterium tuberculosis for the serodiagnosis of tuberculosis, *Agric Biol Chem 55*, 2123-2128.

30. Bourke, J., Brereton, C. F., Gordon, S. V., Lavelle, E. C., and Scanlan, E. M. (2014) The synthesis and biological evaluation of mycobacterial p-hydroxybenzoic acid derivatives (p-HBADs), *Org Biomol Chem 12*, 1114-1123.

31. Barroso, S., Castelli, R., Baggelaar, M. P., Geerdink, D., ter Horst, B., Casas-Arce, E., Overkleeft, H. S., van der Marel, G. A., Codee, J. D., and Minnaard, A. J. (2012) Total synthesis of the triglycosyl phenolic glycolipid PGL-tb1 from Mycobacterium tuberculosis, *Angew Chem Int Ed Engl 51*, 11774-11777.

32. Wei, L., Wei, G., Zhang, H., Wang, P. G., and Du, Y. (2005) Synthesis of new, potent avermectin-like insecticidal agents, *Carbohydr Res 340*, 1583-1590.

33. Wu, X., Marino-Albernas, J. R., Auzanneau, F. I., Verez-Bencomo, V., and Pinto, B. M. (1998) Synthesis and NMR analysis of 13C-labeled oligosaccharides corresponding to the major glycolipid from Mycobacterium leprae, *Carbohydr Res 306*, 493-503.

34. David, S., Thieffry, A., and Veyrières, A. (1981) A mild procedure for the regiospecific benzylation and allylation of polyhydroxy-compounds *via* their stannylene in non-polar solvents, *J Chem Soc Perkin 1*, 1796-1801.

35. Chatterjee, D., Cho, S. N., Brennan, P. J., and Aspinall, G. O. (1986) Chemical synthesis and seroreactivity of O-(3,6-di-O-methyl-beta-D-glucopyranosyl)-(1----4)-O-(2,3-di-O-methyl- alpha-L-rhamnopyranosyl)-(1----9)-oxynonanoyl-bovine serum albumin--the leprosy-specific, natural disaccharide-octyl-neoglycoprotein, *Carbohydr Res 156*, 39-56.

36. Gurjar, M. K., and Saha, U. K. (1993) Sinthesis of the complete glycotetrapeptide core of structurally variant *Mycobacterium fortuitum* glycopeptidolipid, *Bioorg Med Chem Lett 3*, 697-702.

37. Halcomb, R. L., Boyer, S. H., and Danishefsky, S. J. (1992) Synthesis of the calicheamicin aryltetrasaccharide domain bearing a reducing terminus: coupling of fully synthetic aglycone and carbohydrate domains by the Schmidt reaction, *Angew Chem Int Ed Engl 31*, 338-340.

38. Bundle, D. R., and Josephson, S. (1979) Artificial carbohydrate antigens: synthesis of rhamnose disaccharides common to *Shigella flexneri O*-antigen determinants, *Can J Chem 57*, 662-668.

39. Castro-Palomino, J. C., Hernandez-Rensoli, M., and Verez-Bencomo, V. (1996) Synthesis of the trisaccharide a-L-Rha-(1-2)-a-L-Rha-(1-2)-a-L-Rha with a dioxolane-type spacer-arm, *J Carbohydr Chem 15*, 137-146.

40. Abram, C. L., and Lowell, C. A. (2009) The ins and outs of leukocyte integrin signaling, *Annu Rev Immunol 27*, 339-362.

41. Shi, Y., Tohyama, Y., Kadono, T., He, J., Miah, S. M., Hazama, R., Tanaka, C., Tohyama, K., and Yamamura, H. (2006) Protein-tyrosine kinase Syk is required for pathogen engulfment in complement-mediated phagocytosis, *Blood 107*, 4554-4562.

42. Troegeler, A., Lastrucci, C., Duval, C., Tanne, A., Cougoule, C., Maridonneau-Parini, I., Neyrolles, O., and Lugo-Villarino, G. (2014) An efficient siRNA-mediated gene silencing in primary human monocytes, dendritic cells and macrophages, *Immnol Cell Biol 92*, 699-708.

43. Cambier, C. J., Takaki, K. K., Larson, R. P., Hernandez, R. E., Tobin, D. M., Urdahl, K. B., Cosma, C. L., and Ramakrishnan, L. (2014) Mycobacteria manipulate macrophage recruitment through coordinated use of membrane lipids, *Nature 505*, 218-222.

Supporting Information Available: This material is available free of charge on the ACS website. Procedures for the synthesis of PGL epitopes: general procedures and preparation of individual compounds. Physico-chemical data for new compounds: optical rotations, ^{1}H and ^{13}C NMR data, high resolution mass spectra data. Copies of ^{1}H and ^{13}C NMR spectra for new compounds. NMR analysis of PGL purified from rBCG ΔRv2959:: ML0126. Copy of ^{1}H NMR spectra for DIM and PGL purified from rBCG ΔRv2959:: ML0126. Methods, references and supplementary figures.

FIGURE LEGENDS

Figure 1. Structures of PGL produced by various mycobacterial pathogens and construction of the rBCG strains. Structure of the major PGL lipid core (DIM) and the species-specific sugar moieties of the major forms of PGL produced by *M. tuberculosis* (PGL-tb), *M. ulcerans* (PGL-ulc) and *M. leprae* (PGL-1). Genes coding for the enzymes required for the genetic reprogramming of *M. bovis* BCG are indicated.

Figure 2. Analysis of recombinant BCG strains. (A) TLC analysis of lipids extracts from various rBCG producing or not GFP. (B) TLC analysis of glycolipids from rBCG Δ*Rv2959* and rBCG Δ*Rv2959* expressing *ML0126.*

Figure 3. Elaboration of the glycoside building blocks

Figure 4. Synthesis of PGL saccharide epitopes (OS PGLs)

Figure 5. PGL-1 is unique to promote human macrophage invasion *via* the lectin domain of CR3. (A-B) Percentage of infected hMDM after 2h of contact with PGL-expressing rBCG strains at MOI 5:1 was quantified by fluorescence microscopy. (B) Effect of the pre-incubation with 10 μg ml^{-1} blocking anti-CR3 antibodies 2LPM19c or VIM12, or isotype control, on the percentage of infected hMDM. Data are expressed as mean ± SEM and are representative of three independent experiments performed in duplicate. * $P < 0.05$, ** $P < 0.01$

Figure 6. Lyn is required for PGL-1-dependent increase in hMDM uptake. hMDM were transfected with control siRNA or siRNAs targeting Lyn or Syk. 96h after scrambled or siRNA transfection, cell lysates were subjected to Western blot using specific antibodies to assess Lyn and Syk knockdown (A). hMDM were infected with BCG and rBCG-PGL-1 strains at MOI 5:1 for 2h and (B) the percentage of infected hMDM was quantified. Data are expressed as mean ± SEM and are representative of three independent experiments performed in duplicate. ** $P < 0.01$

Figure 7. Binding of PGL-1 to CR3 is mediated by its saccharide domain. (A) Increasing concentrations of purified PGL-1 (B), or purified PGL-1 (5 μM) or its synthetic oligosaccharide moiety (OS-PGL-1) (50 μM), were incubated with immobilized human CR3. Bound PGL-1 was detected using an anti-PGL-1 antibody. (C) Purified CR3 was pre-incubated, or not, with

the synthetic oligosaccharides (OS-PGLs) before being exposed to coated PGL-1. Bound CR3 was detected using an anti-CD11b antibody. Data are expressed as mean ± SEM and are representative of at least 3 independent experiments performed in triplicate. ** $P < 0.01$.

Figure 8. PGL-1 and PGL-tb inhibit TLR-2-induced NF-κB activation and TNF-α secretion. NF-κB-reporter THP-1 cells were infected with PGL-expressing rBCG strains at MOI 1:1 (A) or treated with 5 μM PGL-1, 10 μM DIM or 50 μM synthetic oligosaccharides (OS-PGLs) in the presence of the TLR2 agonist Pam3CSK4 (10 ng ml^{-1}) (C), and phosphatase activity was quantified after 24h. hMDM, either untreated (B) or transfected with control siRNA or siRNAs targeting Lyn or Syk for 96h (F), were infected with PGL-expressing rBCG strains at MOI 10:1 for 2h and the secretion of TNF-α was quantified. (D) HEK-TLR2 NF-κB-reporter cells were treated with the lipids or the OS-PGLs in the presence of Pam3CSK4 at the concentrations indicated above, and phosphatase activity was quantified after 24h. (E) 5 μM purified PGL-1 was incubated with immobilized human TLR2. Bound PGL-1 was detected using an anti-PGL-1 antibody. (A-D,F) Histograms represent the mean ± SEM of at least 3 independent experiments performed in triplicate. * $P < 0.05$; ** $P < 0.01$; *** $P < 0.001$, or (E) are representative of 3 independent experiments performed in triplicate.

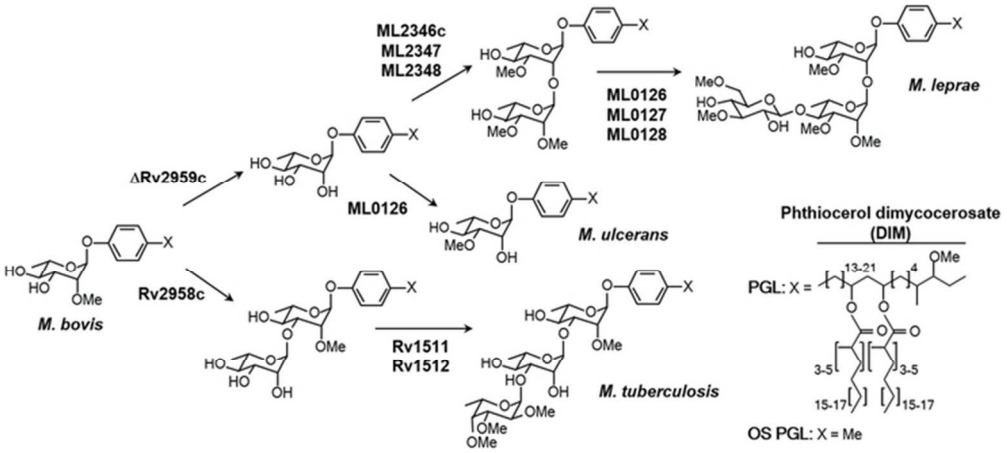

Figure 1. Structures of PGL produced by various mycobacterial pathogens and construction of the rBCG strains. Structure of the major PGL lipid core (DIM) and the species-specific sugar moieties of the major forms of PGL produced by M. tuberculosis (PGL-tb), M. ulcerans (PGL-ulc) and M. leprae (PGL-1). Genes coding for the enzymes required for the genetic reprogramming of M. bovis BCG are indicated.

62x28mm (300 x 300 DPI)

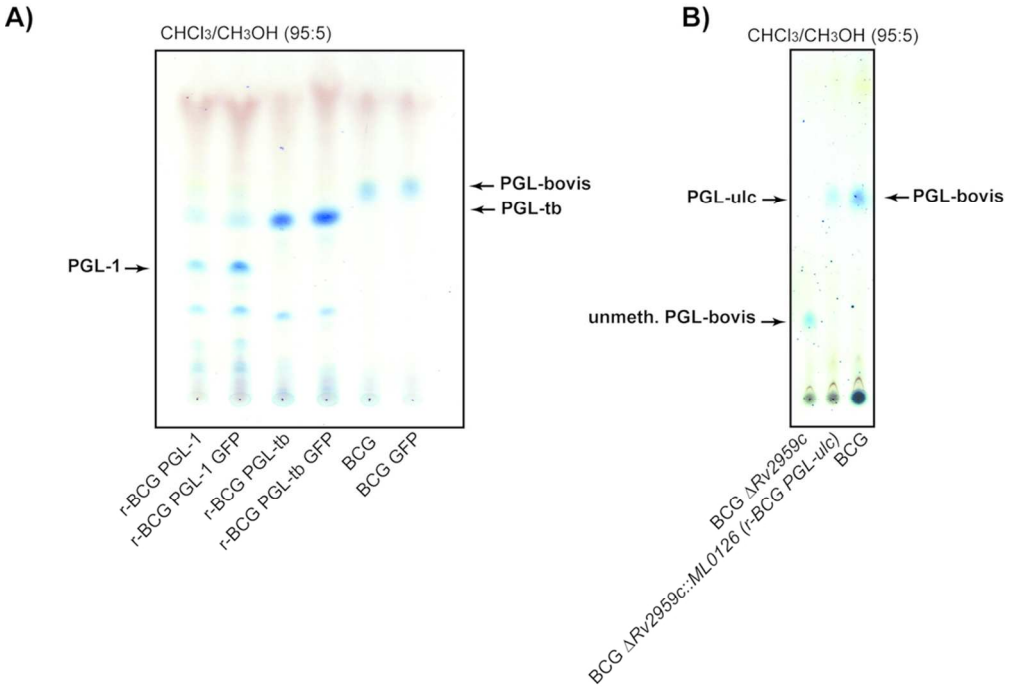

Figure 2. Analysis of recombinant BCG strains. (A) TLC analysis of lipids extracts from various rBCG producing or not GFP. (B) TLC analysis of glycolipids from rBCG ΔRv2959 and rBCG ΔRv2959 expressing ML0126.

96x67mm (300 x 300 DPI)

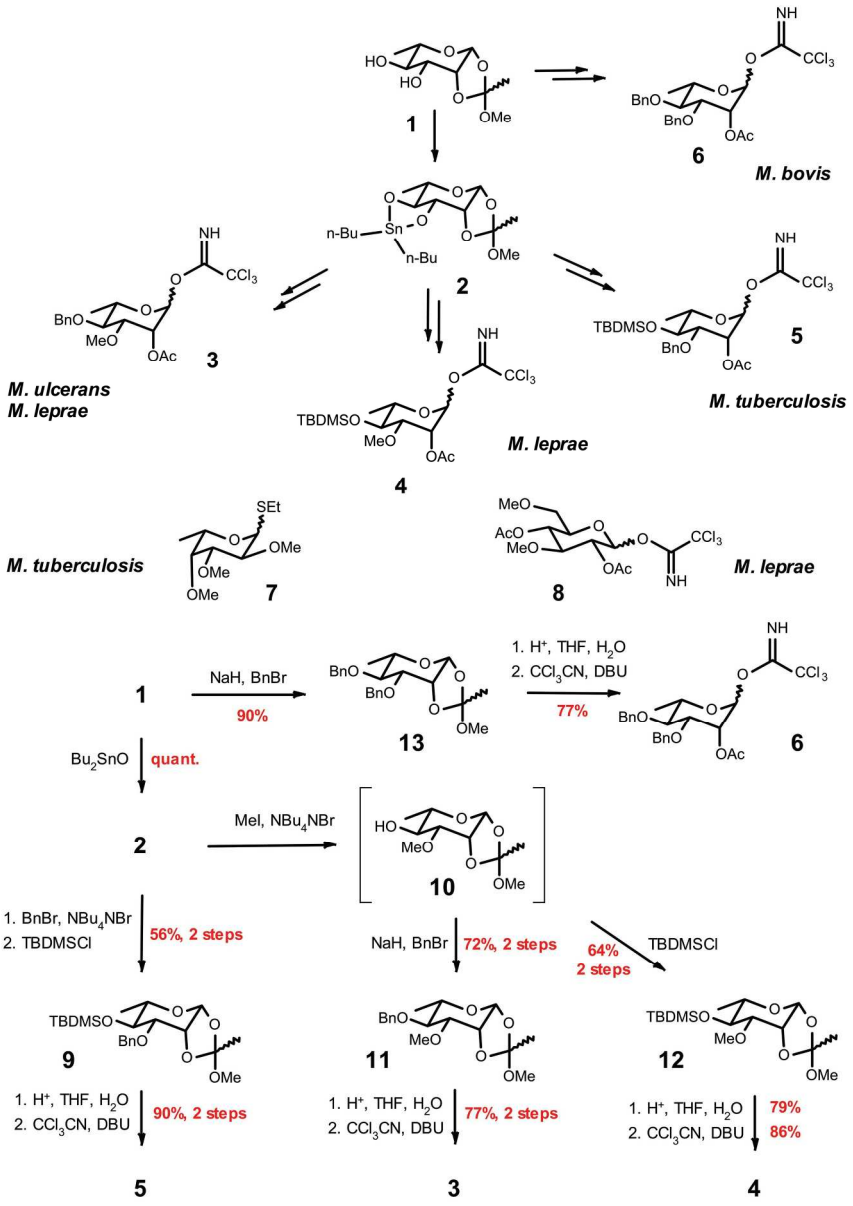

Figure 3. Elaboration of the glycoside building blocks

183x250mm (300 x 300 DPI)

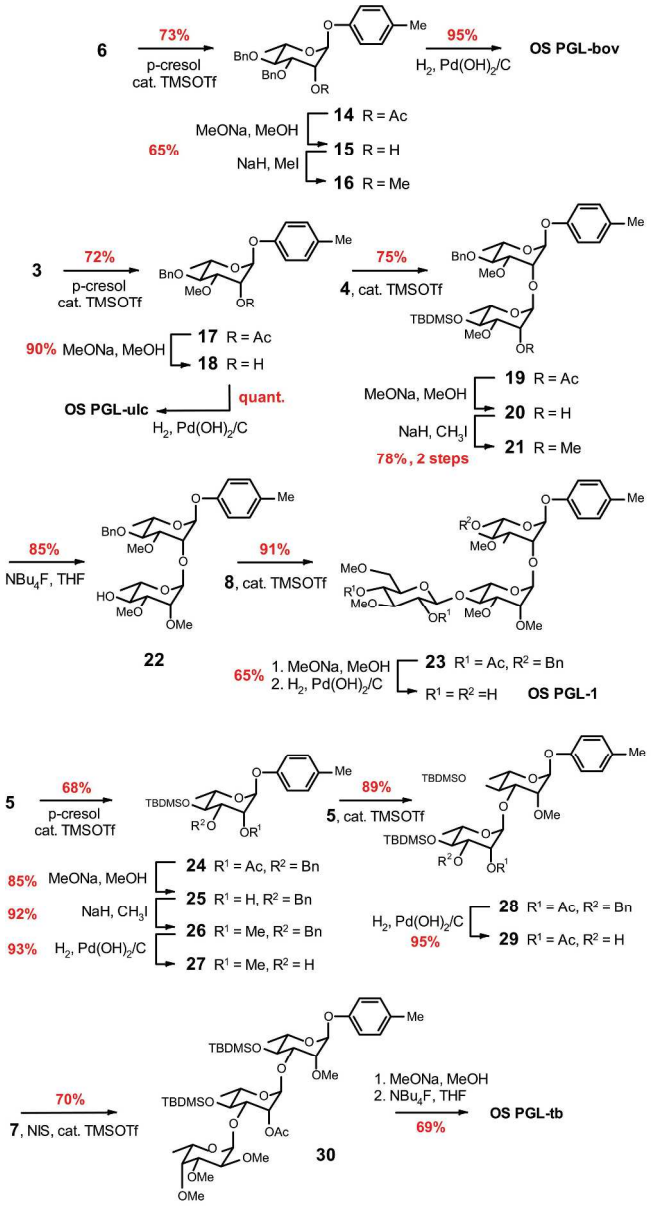

Figure 4. Synthesis of PGL saccharide epitopes (OS PGLs)

221x400mm (300 x 300 DPI)

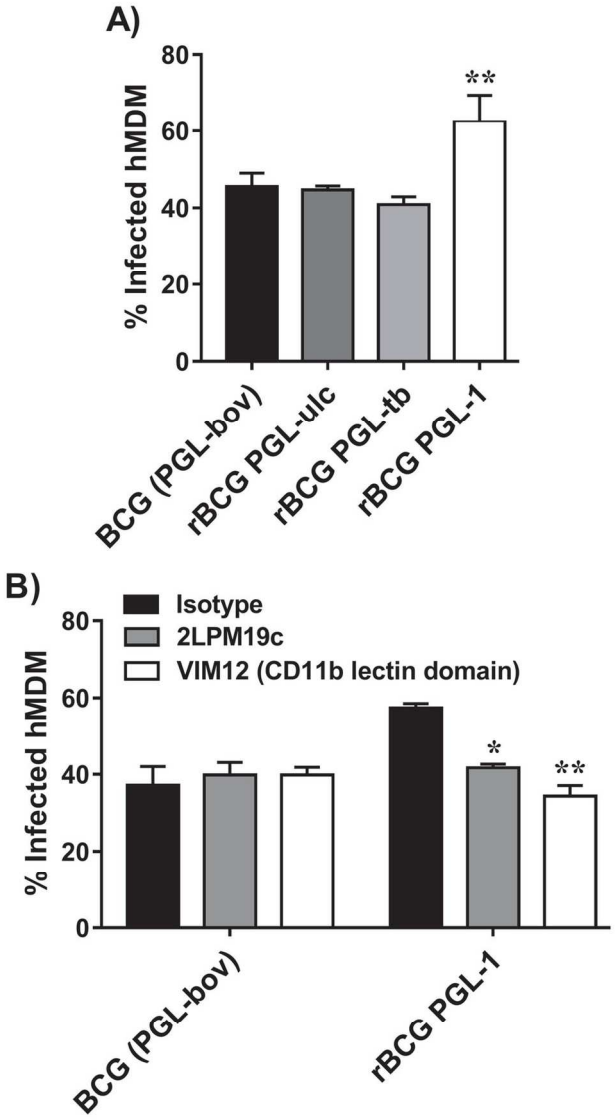

Figure 5. PGL-1 is unique to promote human macrophage invasion via the lectin domain of CR3. (A-B) Percentage of infected hMDM after 2h of contact with PGL-expressing rBCG strains at MOI 5:1 was quantified by fluorescence microscopy. (B) Effect of the pre-incubation with 10 μg ml-1 blocking anti-CR3 antibodies 2LPM19c or VIM12, or isotype control, on the percentage of infected hMDM. Data are expressed as mean ± SEM and are representative of three independent experiments performed in duplicate. * $P < 0.05$, ** $P < 0.01$

101x177mm (300 x 300 DPI)

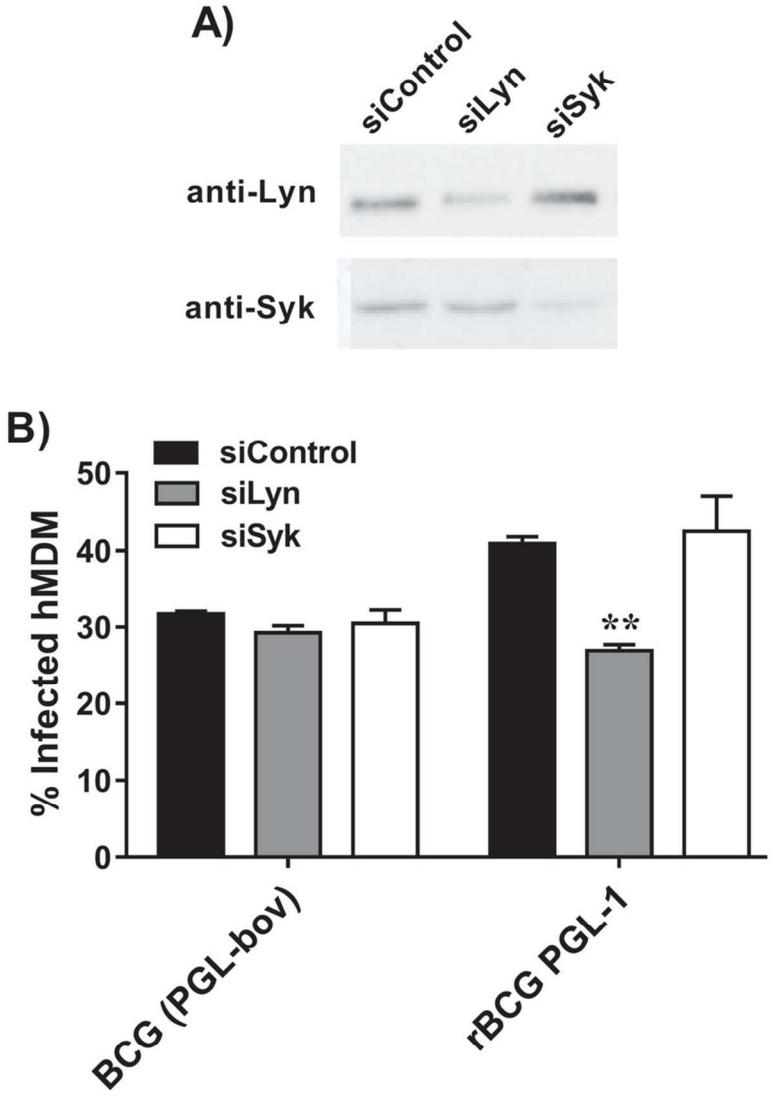

Figure 6. Lyn is required for PGL-1-dependent increase in hMDM uptake. hMDM were transfected with control siRNA or siRNAs targeting Lyn or Syk. 96h after scrambled or siRNA transfection, cell lysates were subjected to Western blot using specific antibodies to assess Lyn and Syk knockdown (A). hMDM were infected with BCG and rBCG-PGL-1 strains at MOI 5:1 for 2h and (B) the percentage of infected hMDM was quantified. Data are expressed as mean ± SEM and are representative of three independent experiments performed in duplicate. ** $P < 0.01$

81x113mm (300 x 300 DPI)

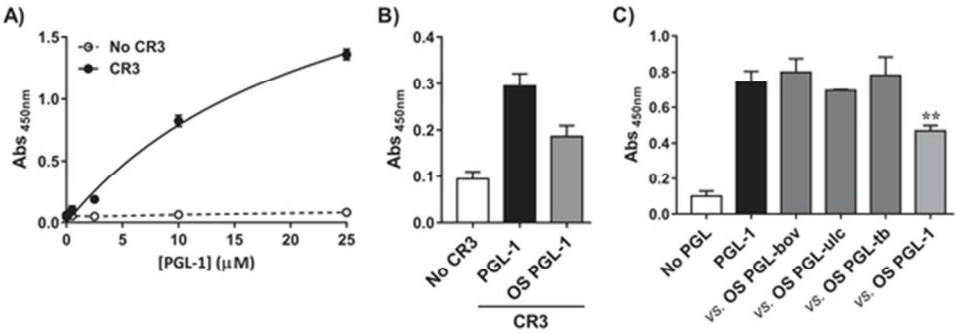

Figure 7. Binding of PGL-1 to CR3 is mediated by its saccharide domain. (A) Increasing concentrations of purified PGL-1 (B), or purified PGL-1 (5 μM) or its synthetic oligosaccharide moiety (OS-PGL-1) (50 μM), were incubated with immobilized human CR3. Bound PGL-1 was detected using an anti-PGL-1 antibody. (C) Purified CR3 was pre-incubated, or not, with the synthetic oligosaccharides (OS-PGLs) before being exposed to coated PGL-1. Bound CR3 was detected using an anti-CD11b antibody. Data are expressed as mean ± SEM and are representative of at least 3 independent experiments performed in triplicate. ** $P < 0.01$.

52x19mm (300 x 300 DPI)

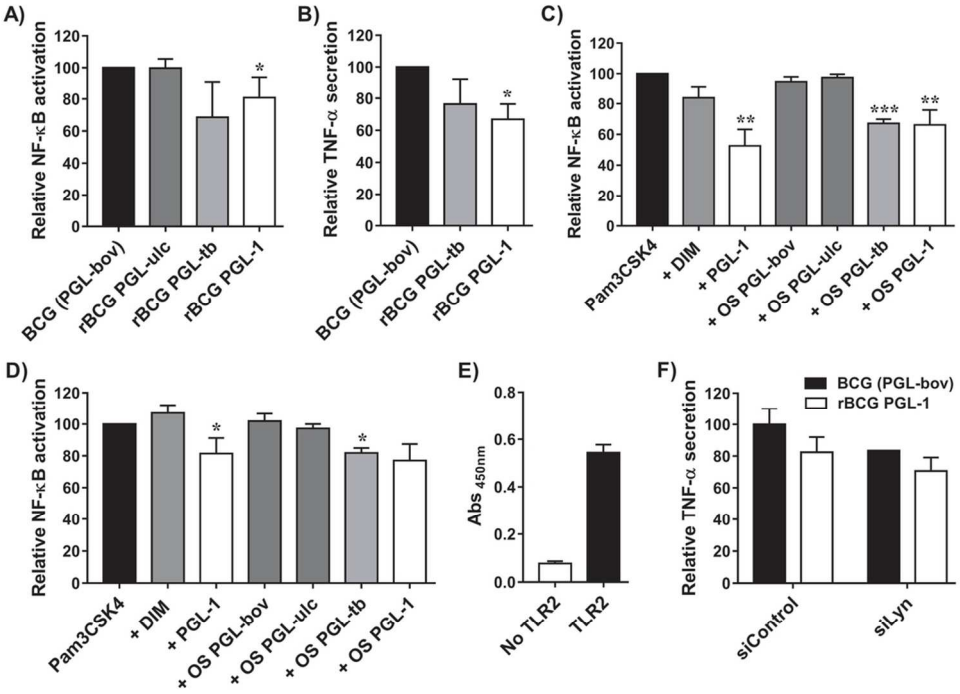

Figure 8. Both PGL-1 and PGL-tb inhibit TLR-2-induced NF-κB activation and TNF-α secretion. NF-κB-reporter THP-1 cells were infected with PGL-expressing rBCG strains at MOI 1:1 (A) or treated with 5 μM PGL-1, 10 μM DIM or 50 μM synthetic oligosaccharides (OS-PGLs) in the presence of the TLR2 agonist Pam3CSK4 (10 ng ml-1) (C), and SEAP activity was quantified after 24h. hMDM, either untreated (B) or transfected with control siRNA or siRNAs targeting Lyn or Syk for 96h (F), were infected with PGL-expressing rBCG strains at MOI 10:1 for 2h and the secretion of TNF-α was quantified. (D) HEK-TLR2 NF-κB-reporter cells were treated with the lipids or the OS-PGLs in the presence of Pam3CSK4 at the concentrations indicated above, and SEAP activity was quantified after 24h. (E) 5 μM purified PGL-1 was incubated with immobilized human TLR2. Bound PGL-1 was detected using an anti-PGL-1 antibody. (A-D,F) Histograms represent the mean ± SEM of at least 3 independent experiments performed in triplicate. * $P < 0.05$; ** $P < 0.01$; *** $P < 0.001$. (E) Data are expressed as mean ± SEM and are representative of 3 independent experiments performed in triplicate.

101x75mm (300 x 300 DPI)

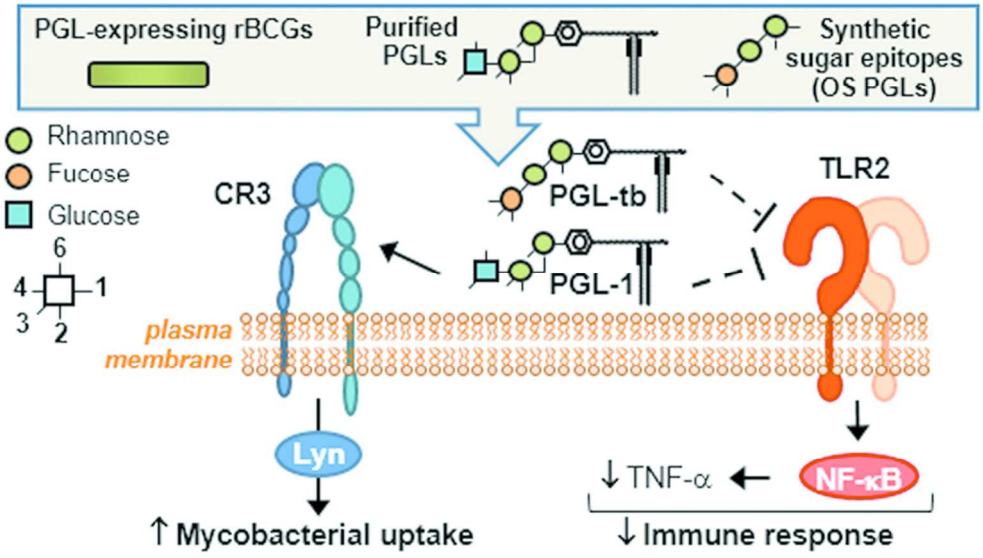

TOC graphic

80x44mm (300 x 300 DPI)